

# DEVELOPMENT OF COMPACT FFAG ACCELERATOR FOR HEAVY ION RADIOTHERAPY

T. Misu, S. Yamada, M. Kanazawa, Y. Iwata, S. Hojo, A. Sugiura, N. Miyahara, M. Muramatsu, T. Murakami, K. Noda, E. Takada, T. Fujisawa, M. Kumada, T. Honma, T. Furukawa, Y. Sato, M. Torikoshi, A. Kitagawa, K. Kono, Y. Sakamoto, M. Suda, M. Yoshimoto, NIRS, Chiba, Japan

## Abstract

In recent years successful clinical trials at Heavy Ion Medical Accelerator in Chiba (HIMAC) have proven the heavy-ion accelerator to be a powerful tool for cancer treatment. Based on our satisfactory clinical records at HIMAC [1], we plan to propose a compact, cost-effective medical Fixed-Field Alternating-Gradient (FFAG) accelerator to establish the medical standards for a carbon-beam cancer therapy. In this study we present our current accelerator design scheme.

## 1 INTRODUCTION

Operation of the HIMAC in recent years has led to significant research contributions in fundamental physics, radiation biology, and trial carbon-beam therapy. In cancer therapy, HIMAC has shown its effectiveness over conventional radiation therapy for treating critically located tumors in a much more controlled manner. With the successful results of carbon-beam radiotherapy at HIMAC, the next phase of developmental studies has been initiated under the Advanced Compact Accelerator Development (ACAD) Project to promote the heavy-ion cancer treatment throughout the nation. We are currently investigating the possible use of a compact medical accelerator based on Fixed-Field Alternating-Gradient (FFAG) principle, which is believed to have some advantages over conventional synchrotrons. For instance, while the repetition rate of a conventional synchrotron is limited by the time required for the pulsed magnetic field cycle, an FFAG machine is free from such a restriction because of its time-independent field structure; this leads to higher beam intensity.

The present overall specification of a medical FFAG accelerator is the following:

Particle: Carbon

Injection Energy: 40 keV/u (Br=0.086 Tm)

Extraction Energy: 400 MeV/u (Br=6.34 Tm)

Number of Particles:  $2 \times 10^9$  pps

Repetition Rate: over 100 Hz

## 2 SYSTEMATIC ANALYSIS OF FFAG SCHEME

It is well-known that the most practical FFAG schemes are the radial and spiral sector configurations. Several in-depth studies on FFAG ring have been conducted [2,3], and the optical properties of FFAG have been established in theoretical sense. However, very few FFAG machines

have actually been constructed [2,4], and its physical characteristics are not yet fully understood. Keeping in mind the main theme of this project, the compact FFAG lattice structure suitable for popularization is investigated.

### 2.1 Optical Model

In order to carry out systematic analysis on FFAG for minimal design, one can generalize its lattice structure in terms of three basic elements as in Fig. 1.

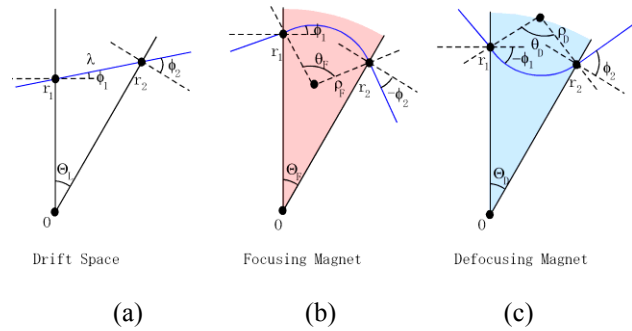


Fig. 1 Basic Elements of FFAG

Here,  $\Theta_L$ ,  $\Theta_F$  and  $\Theta_D$  are the open angles of drift space, focusing (F) and defocusing (D) magnets;  $\theta_F$  and  $\theta_D$  are the bending angles of F and D magnets;  $r_1$  and  $r_2$  are the distances from the center of the machine to the beam orbit at each boundary;  $\phi_1$  and  $\phi_2$  are the angles between the beam orbit and a normal vector at each boundary.

Since the size of a circular accelerator depends on its maximum magnetic field strength, one can define reduced parameters with respect to the radius of curvature at maximum field strength, denoted by  $\rho_0$ . For each optical element in the radial sector type, these reduced parameters can be deduced in the following relations:

#### ● Focusing Magnet

$$\varepsilon_1 = \phi_1; \varepsilon_2 = \theta_F - \phi_1 - \Theta_F; \phi_2 = -\varepsilon_2$$

$$\frac{r_1}{\rho_0} = \left\{ \frac{1}{\tan \Theta_F} [\sin \phi_1 + \sin(\theta_F - \phi_1)] + [\cos \phi_1 - \cos(\theta_F - \phi_1)] \right\} \left( \frac{\rho_F}{\rho_0} \right)$$

$$\frac{r_2}{\rho_0} = \frac{1}{\sin \Theta_F} \left( \frac{\rho_F}{\rho_0} \right) [\sin \phi_1 + \sin(\theta_F - \phi_1)]$$

#### ● Defocusing Magnet

$$\varepsilon_1 = -\phi_1; \varepsilon_2 = \theta_D + \phi_1 + \Theta_D; \phi_2 = \varepsilon_2$$

$$\frac{r_1}{\rho_0} = \left\{ \frac{1}{\tan \Theta_D} [\sin(\theta_D + \phi_1) - \sin \phi_1] + [\cos(\theta_D + \phi_1) - \cos \phi_1] \right\} \left( \frac{\rho_D}{\rho_0} \right)$$

$$\frac{r_2}{\rho_0} = \frac{1}{\sin \Theta_D} [\sin(\theta_D + \phi_1) - \sin \phi_1] \left( \frac{\rho_D}{\rho_0} \right)$$

● Drift Space

$$\phi_2 = \Theta_L + \phi_1$$

$$\frac{r_1}{\rho_0} = \left\{ \frac{\cos \phi_1 [1 - \tan \Theta_L \tan \phi_1]}{\tan \Theta_L} \right\} \left( \frac{\lambda}{\rho_0} \right)$$

$$\frac{r_2}{\rho_0} = \frac{1}{\cos \Theta_L (1 - \tan \Theta_L \tan \phi_1)} \left( \frac{r_1}{\rho_0} \right)$$

where  $\varepsilon_1$  and  $\varepsilon_2$  are the edge angles at element boundary. Therefore, any arbitrary order of these elements can be placed and expressed in terms of the above parameters. If we label all the elements in order from 1 to  $n$ , its closed orbit can be found by imposing  $r_2/\rho_0|_i = r_1/\rho_0|_{i+1}$  ( $i$  corresponds to the  $i$ th element) and  $r_2/\rho_0|_n = r_1/\rho_0|_1$ .

For the spiral sector type with spiral angle  $\xi$ , its closed orbit can be obtained by simply replacing the above edge angles by

$$\varepsilon_1 \rightarrow \varepsilon_1 + \sigma_M \cdot \xi \text{ and } \varepsilon_2 \rightarrow \varepsilon_2 - \sigma_M \cdot \xi$$

where  $M$  denotes F or D magnet;  $\sigma_F = 1$  and  $\sigma_D = -1$ .

In terms of the above generalized expressions for both radial and spiral sector FFAG accelerators, F-D combined spiral sector configuration can also be designed in principle. Once the closed orbit of an arbitrary configuration is determined, its accelerator size can be measured by the circumference factor  $\langle r \rangle / \rho_0$  as

$$\frac{\langle r \rangle}{\rho_0} = \sum_i^{N_F} \left( \frac{\rho_F}{\rho_0} \right)_i \theta_{F|i} + \sum_i^{N_D} \left( \frac{\rho_D}{\rho_0} \right)_i \theta_{D|i} + \sum_i^{N_A} \left( \frac{\lambda}{\rho_0} \right)_i$$

## 2.2 Stability and Accelerator Size

Once the cell number, the lattice order and the field index are specified for radial sector type, all the necessary lattice parameters can be determined in three-dimensional parameter space, e.g., in terms of  $\theta_F$ ,  $\Theta_F$  and  $\Theta_L$ . In the following, the three-dimensional parameter space was searched under the conditions leading to small ring size,

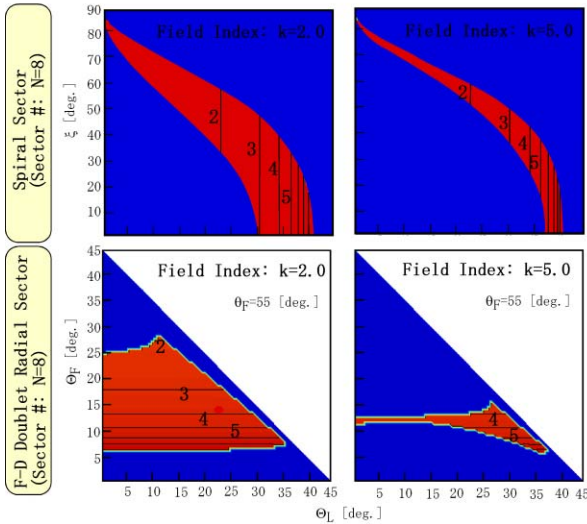


Fig. 2 Typical stability diagrams for spiral and radial sector FFAG lattices. Stability regions are shaded in red, and contour lines correspond to circumference factor  $\langle r \rangle / \rho_0$ . Top: Spiral sector type. Bottom: Radial sector type with F-D doublet.

short orbit excursion, small magnet size, and large drift space. Some of the typical stability diagrams for spiral and radial sector lattices are presented in Fig. 2.

Due to the fact that the spiral sector type requires complex magnet shapes and the RF cavity cannot be easily placed in spiral shaped drift space, the following discussion is limited to the radial sector FFAG with positive field index only. It is obvious from the figure that the increasing field index  $k$  leads to stability region reduction and the increased accelerator size. In general, the total size of a whole accelerator remains small when minimizing the circumference factor, whereas the orbit excursion cannot simply be reduced by increasing the field index  $k$  or increasing the cell number. To illustrate this point, the maximum amount of drift space for given values of accelerator size are compared in Fig. 3a.

To achieve higher  $k$  values, one cannot avoid an increase in accelerator size  $\langle r \rangle / \rho_0$ . Although the orbit excursion normalized by the accelerator radius decreases for increasing field index  $k$ , as explicitly written in terms of momentum ratio

$$\left( \frac{\langle r_{ext} \rangle - \langle r_{inj} \rangle}{\langle r_{ext} \rangle} \right) = 1 - \left( p_{inj} c / p_{ext} c \right)^{\frac{1}{k+1}},$$

the minimal accelerator size increases for larger values of  $k$ , as shown in Fig. 3b. Other combined radial sector lattices like D-F-D triplet and F-D-F triplet were also analyzed and show a similar tendency.

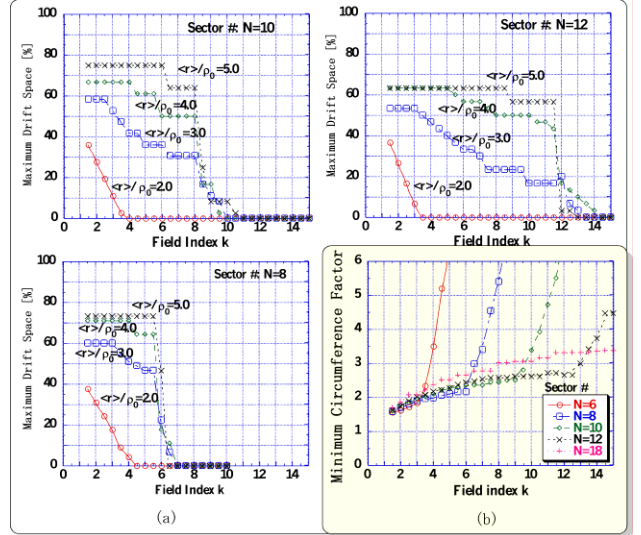


Fig. 3 (a) the maximum drift space for given circumference factor and (b) the minimum accelerator radius for a given cell number are shown as a function of field index  $k$ . Only the F-D doublet radial sector type is displayed.

## 2.3 Minimal FFAG Configuration

By imposing sufficient drift space for placing RF cavities and injection/extraction elements, the circumference factor of a minimal configuration can be set around 3 with field index of 5-10 and the cell number of 8-12. To design a compact radial sector FFAG machine, let us propose the F-D doublet radial sector FFAG of 8 cells with field index of 5.0, see Fig. 4.

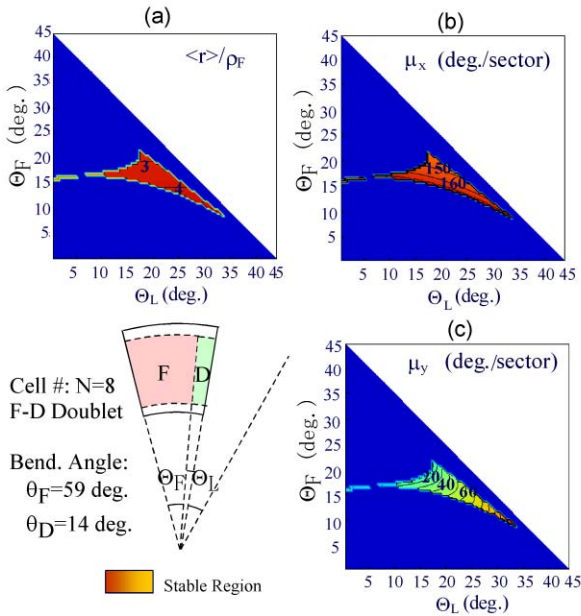


Fig. 4 Stability Diagrams for F-D doublet radial sector FFAG. Cell number of 8 and field index of 5.0 are chosen. Contour lines correspond to (a) circumference factor, (b) horizontal phase shift, and (c) vertical phase shift calculated for  $k=5$ . Stability regions are obtained for  $\rho_F \leq \rho_D$  only.

### 3 PRESENT FFAG DESIGN SCHEME AND ITS PROSPECTIVES

Based on the above systematic analysis, we can construct FFAG lattices. The schematic view of the 400 MeV/u carbon-beam FFAG is shown in Fig. 5; its betatron and dispersion functions are displayed in Fig. 6. Here, a lattice structure of 8 sectors with large drift space was chosen and modified to superperiod of 4 for reserving a larger drift space for extraction components. In this scheme, the 2-stage cascade acceleration is assumed temporarily; a booster FFAG accelerates a beam of  $C^{4+}$  from 40 keV/u to 20 MeV/u; a main FFAG ring delivers  $C^{6+}$  in the energy range of 20 – 400 MeV/u.

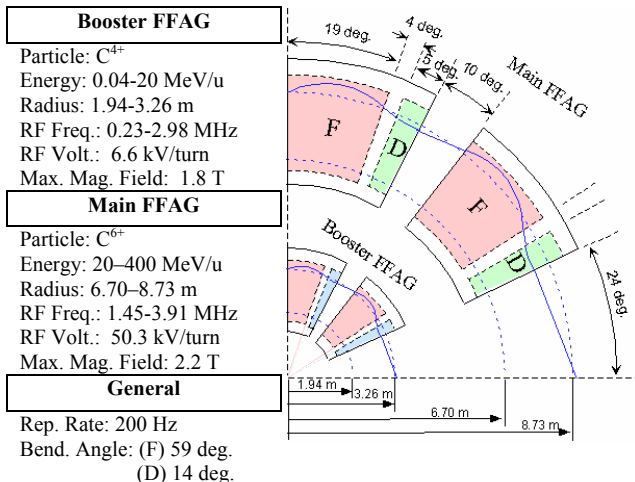


Fig. 5 Schematic configuration of the 2-stage FFAG

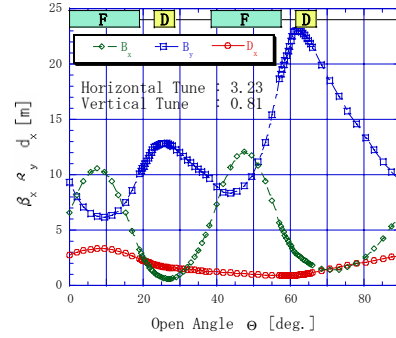


Fig. 6 The betatron and dispersion functions of the lattice given in Fig. 5 are calculated at extraction radius.

However, the present lattice structure still requires large orbit excursion of about 2m. Such a large excursion creates some technical problems: the fringing field produced by sector magnets gives rise to severe vertical tune shift, the larger RF core size is not efficient in producing higher shunt impedance, and the extremely thick chamber between magnet poles is necessary. We are currently in the process of remodelling and optimising its lattice structure.

### 4 CONCLUSION

For the popularization of carbon-beam therapy, we have just started the developmental studies on a compact FFAG accelerator. At present, a F-D doublet radial sector type with  $N=8$  and  $k=5.0$  is assumed as a possible candidate. Since the voltage gain per turn at RF cavity becomes a key to achieving higher repetition rate, we are currently considering the possible use of a low-Q FINEMET-loaded cavity that has recently been developed at KEK [5]. The low-Q cavity with the extremely high permeability of FINEMET core makes non-resonant acceleration possible. Within the next four years of the ACAD Project, a scaled-down version of a prototype FFAG accelerator will be constructed for testing developmental elements.

This research work was supported in part by the Japan Ministry of Education, Culture, Sports, Science and Technology, under the ACAD project, and authors would like to express cordial thanks to the members of NIRS and KEK for their endurance and guidance.

### 5 REFERENCES

- [1] S. Yamada, Paper submitted to APAC01, Beijing, China, Sept. 17-21 (2001)
- [2] E. T. Cole, et al., Rev. Sci. Instr. **28**(1957)403
- [3] R. L. Kustom, et al., IEEE Vol. NS-32 (1985)2672
- [4] Y. Mori, et al., Proc. 12<sup>th</sup> Symp. Acc. Sci. Tech., Wako, Japan (1999)81
- [5] T. Uesugi, et al., Proc. 11<sup>th</sup> Symp. Acc. Sci. Tech., Nishiharima, Japan (1997)188